Vol. 56: 147–155, 2013
doi: 10.3354/cr01150

CLIMATE RESEARCH
Clim Res

Published online March 26

Climate responses to historical land cover changes

Ye Wang[1,2,*], Xiaodong Yan[2,3]

[1]College of Civil Aviation, Nanjing University of Aeronautics and Astronautics, Nanjing 210016, PR China
[2]Key Laboratory of Regional Climate-Environment for East Asia, Chinese Academy of Sciences, Beijing 10029, PR China
[3]State Key Laboratory of Earth Surface Processes and Resource Ecology (ESPRE), College of Global Change and Earth System Science, Beijing Normal University, 19 Xinjiekouwai Street, Haidian District, Beijing 100875, PR China

ABSTRACT: This study assessed the biogeophysical effects of land cover change on climate using MPM-2 during the past millennium. Simulations based on the Climate and Environmental Retrieval and Archive (CERA) land cover dataset were carried out to equilibrium from AD 800 to 2000 after a spin-up time of 5300 yr. We concluded that there was a cooling biogeophysical effect of about 0.13°C in global mean annual temperature in response to historical deforestation, with a maximum cooling of 0.5°C over Eurasia and a minimum cooling of 0.02°C at low latitudes over the Southern Hemisphere. Much larger contrasts were found on a seasonal scale, while these changes were largely offset on an annual scale. Seasonally, cooling occurred in the middle northern latitudes and warming occurred in the low southern latitudes due to historical deforestation. The effect of land cover change was most pronounced over Eurasia, with a maximum cooling of approximately 0.8°C at middle latitudes during summer and a maximum warming of 0.1°C at low latitudes over the Southern Hemisphere during the Northern Hemisphere summer, owing to the changes in albedo and precipitation. These results suggest that changes in land cover triggered a chain of feedbacks in the climate system, and they highlight the need for further research in this area.

KEY WORDS: Biogeophysical effects · Climate change · Land cover change · Earth system model at intermediate complexity · EMIC · Modeling

1. INTRODUCTION

Humans have altered the land cover surface significantly over the last few millennia by transforming the natural ecosystem into anthropogenically managed areas. The biogeophysical mechanisms through which the changes in land cover affect climate include the effects of changes in surface albedo, roughness and soil hydrology. Many studies have demonstrated these effects and simulated their causes (e.g. Brovkin et al. 1999, Betts 2001, Bertrand et al. 2002, Bauer et al. 2003, Gao et al. 2003, Zhang et al. 2005, Gao et al. 2007, Nair et al. 2007, Anav et al. 2010, Davin & de Noblet-Ducoudré 2010, Pielke et al. 2011, Pitman et al. 2011, Avila et al. 2012, Lawrence et al. 2012). Over the last millennium biogeophysical mechanisms due to land cover changes have caused a global cooling of approximately 0.35°C, which is most pronounced in the northern mid-high latitudes (Brovkin et al. 1999). Other researchers have also revealed an averaged global cooling effect in response to increased albedo from land conversion (Bonan 1997, 1999, Govindasamy et al. 2001).

Using a general circulation model (GCM), De Fries et al. (2002) found that the dominant effect of deforestation appeared to be physiological rather than from increased albedo, resulting in increasing sensible heat relative to latent heat flux for a warming effect in the tropics and subtropics. Bounoua et al. (2002), in deforestation experiments with a GCM coupled to the simple Biosphere Model (SiB2), showed that conversion (mainly the replacement of forest with crops) cooled canopy temperatures up to 0.7°C in summer and 1.1°C during winter in temper-

*Email: wytea@126.com

ate latitudes, while in the tropics and subtropics conversion warmed canopy temperature by about 0.8°C year round. The boreal forest warmed both winter and summer air temperatures, relative to simulations in which the forest was replaced with bare ground or tundra vegetation within numerical experiments using the National Center for Atmospheric Research's (NCAR) climate model CCM1 (Bonan et al. 1992). Using HadAM3, Betts (2001) found that global temperature was only −0.02°C cooler in a comparison between present-day and pre-industrial vegetation equilibrium, but noted stronger cooling (in the range of −1 to −2°C) in the northern mid-latitudes in winter and spring. Chase et al. (2000), in experiments with NCAR CCM3 with prescribed surface seawater temperatures (SST), obtained a global temperature warming of 0.05°C in winter in the north. Recently, sensitivity experiments performed with a regional climate model, Version 4 (RegCM4), indicated that expanding agriculture into forested areas led to a modest reduction in monthly rainfall totals and also may contribute to notable shifts in moisture convergence zones and centers of rainfall maxima (Otieno & Anyah 2012). However, while the global cooling effects of historical deforestation could be modeled explicitly, the seasonal response of climate to historical land cover change was less certain. In addition, most seasonal climate responses to land cover change have been simulated with atmospheric general circulation models (AGCMs) without interactive ocean models, while in reality climate changes induced by land cover changes are affected by feedbacks with SST and sea ice, and even with thermohaline circulation of the ocean. So further studies on climate changes due to deforestation are still necessary. In this study, a consistent time evolution of global land use at spatially explicit resolutions covering the entire last millennium (Pongratz et al. 2008) was used to simulate the climate response to historical land cover change.

To allow long-term model integrations and simulate responses with interactive components of the Earth's system, we used an Earth system model of intermediate complexity (EMIC) — MPM-2 (Fanning & Weaver 1996, Wang & Mysak 2000) — to study the biogeophysical effects of historical land cover changes on climate and their seasonal effects. EMICs provide a comprehensive, geographically explicit explanation of the earth's system, including almost all of its components. Although it moderately simplifies the courses and details using parameterization, it embodies the feedbacks and interactions among components of the climate system. So EMICs can simulate climate change on large time scales. The computational efficiency of these models allows the performance of many sensitivity experiments, as well as investigation of the influence of uncertainty in climatic forcings and process parameterizations on model results (Forest et al. 2002).

The purpose of this paper was to analyze the biogeophysical effects of historical land cover change on the earth during the last millennium using MPM-2, and in particular, to assess seasonal responses of the climate system to land cover change.

2. MATERIALS AND METHODS

To analyze the biogeophysical effects of historical land cover change, the McGill Paleoclimate Model-2 (MPM-2) (Fanning & Weaver 1996), an EMIC, was employed. The MPM-2 is a global climate model, which consists of a 2-dimensional energy and moisture balance atmosphere model, a multi-basin zonally averaged dynamic ocean model based on vorticity conservation, a dynamic ice sheet model, a zero-layer thermodynamic–dynamic sea ice model without snow, and a land surface model in which the surface temperature is predicted using the energy balance equation. The MPM-2 was also interactively coupled to the dynamical vegetation model VECODE (Semtner 1976), which is based on a continuous bioclimatic classification that provides the relative cover of trees, grass and potential desert for each continent and latitude (Brovkin et al. 1997). MPM-2 has successfully simulated changes in the thermohaline circulation state (Wang & Mysak 2001, Wang et al. 2002) and the last glacial inception (Z. Wang et al. 2005). Furthermore, MPM-2 has also successfully simulated the climate changes since the beginning of the Holocene, such as temperature, precipitation and vegetation distribution (Y. Wang et al. 2005).

To assess the effects of land cover change on climate, the dataset used was a reconstruction of that provided by Pongratz et al. (2008) for CERA (hereafter the CERA dataset). The reconstruction is based on published maps of agricultural areas over the last 3 centuries. For earlier times, with the country-based method of using population data as a proxy for agricultural activity, the extent of cropland and pasture is consistently simulated for the period since AD 800. The reconstruction shows that global land cover change was minor between AD 800 and 1700 compared to that occurring during industrial times. Compared to previous millennia, however, land cover change during the pre-industrial time period of the

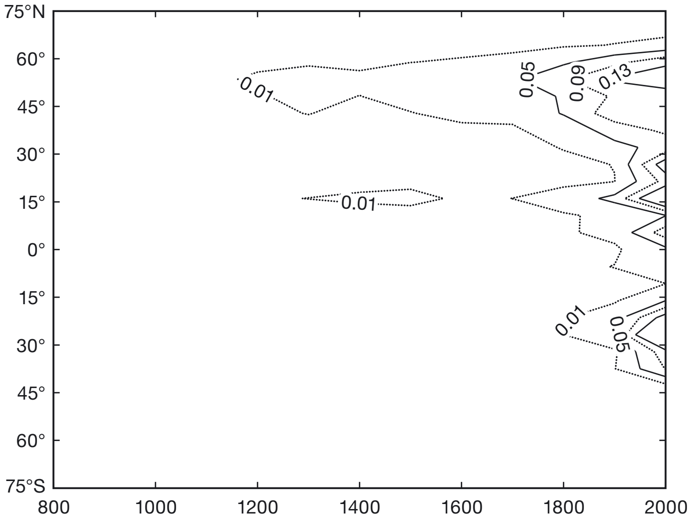

Fig. 1. Zonally averaged changes in the grassland fraction from AD 800 to 2000

last millennium must have been large, and notable fluctuations and distinct histories of agriculture are revealed on regional scales (Pongratz et al. 2008).

This dataset consists of the global coverage of 3 human use types (crop, C3 and C4 pasture) and 11 natural vegetation types, at a 30 min resolution. For each year, a map is provided that contains 14 fields. Each field holds the fraction (between 0 and 1) that the respective vegetation type covers in the total grid cell. Zonally averaged expansion in the grassland fraction is shown in Fig. 1. The grassland expansion from AD 800 to 1700 is minor compared with that from AD 1700 to 2000 (Fig. 1). The Northern Hemisphere (NH) mid-latitudes have experienced rapid grassland expansion since AD 1700.

To investigate the effects of land cover change, we performed a simulation with the historical deforestation dynamics (land cover changes) in which the model was run from AD 800 to 2000 under a pre-industrial CO_2 concentration of 280 ppm. Earth orbital parameters were kept constant at present-day values. In order to obtain the same initial conditions, we integrated our simulation to equilibrium from AD 800 to 2000 after a spin-up time of 5300 yr. Note: This is a sensitivity study not a hindcast prediction. We followed Pitman et al. (2009) and Findell et al. (2007) in using a modified Student's *t*-test (Zwiers & von Storch 1995) to compare differences between results at each model grid cell. This test is more rigorous than the standard *t*-test because it accounts for auto-correlation within time series, reducing the rate of false positives (Pitman et al. 2009).

3. RESULTS

3.1. The response of Northern Hemisphere temperatures and sea ice area to historical land cover changes

The experiment resulted in an average cooling of 0.13°C globally, due to land cover changes during the last millennium, with a more prominent cooling of −0.21°C over the NH. These changes were caused primarily by increases in surface albedo that led to negative radiative forcing. Land cover in the NH has suffered more serious deforestation than that in the Southern Hemisphere (SH) over the last millennium (as indicated by changes in the grassland fraction in Fig. 1). In addition, landmass area is greater in the NH, and this responds more rapidly to external climatic forcings (e.g. changes in solar radiation or CO_2 concentration) than does the thermally inert ocean

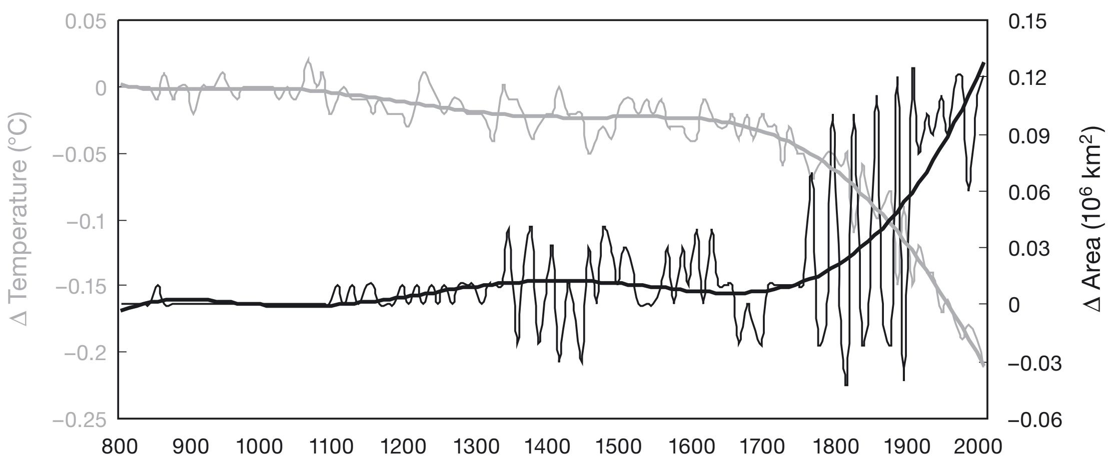

Fig. 2. Changes in mean temperature (gray) and sea ice area (black) for the Northern Hemisphere. Thick lines: trend lines

(Brovkin et al. 2006). Consequently, the cooling effect of land cover changes on climate was more prominent in the NH. The NH long-term cooling trend for the simulation is shown clearly in Fig. 2. Before AD 1700, changes in temperature due to deforestation were rather small (less than –0.1°C); these accelerated after 1700, reaching a maximum of 0.21°C in 2000. The trend can be accounted for by both the temporal dynamics of the land cover changes and the sea ice nonlinear response. The NH sea ice area increased while temperature decreased (in Fig. 2). Oscillations in the temperature response to monotonous deforestation forcing were generated by the sea ice. A significant nonlinear response of temperature to land cover changes has been suggested and could be explained by the positive feedback of sea ice. As a result of reduction in temperature, the sea ice cover expanded, which led to a decrease in absorbing short-wave radiation, and may have affected SST and sea ice, and even thermohaline circulation. A decline of 0.21°C in NH temperatures is indicated finally in the year 2000. The correlation of NH temperatures and sea ice area was –0.8. Although the variability of sea ice seems to have been increasing wildly since about 1800, temperature variability seems to have decreased during the same period. This accounts for the discontinuity in sea ice changes and the nonlinear response of NH sea ice to NH temperatures. This nonlinear response also affected NH temperatures. The results suggest that the potential influence of land cover changes could be significant, owing to the nonlinear response of temperature to land cover change, which should receive more attention.

3.2. The seasonal response of temperature and albedo to historical land cover changes

Since the changes in land cover primarily affected climate through changes in surface albedo and soil hydrology, which vary seasonally, it was important to compare their net seasonal effects. So the seasonal responses of temperature and albedo to historical land cover changes were analyzed.

Considering the Land Use and Land Cover Change (LUCC) over land, the results over land only were focused on assessing the climate response to land cover changes. There were marked seasonal differences in the magnitude of cooling in response to land cover changes (Fig. 3). In Fig. 3, we only show results that were statistically significant at the 95% level. For annual and spring temperature changes (Fig. 3a,b), all grid cells were statistically significant. This can be accounted for by advection in MPM-2, which was parameterized. Even heat transportation of the ocean was heavily dependent on parameterization. Such parameterization causes widespread climate change; this is different from large local changes in climate in other studies owing to the influence of advection (Pitman et al. 2009). For summer and winter temperature changes (Fig. 3c,d) most grid cells were also statistically significant. Because of the prominent temperature change, advection was influenced significantly in MAM (March, April and May). Furthermore, the largest anomalies occurred over land in summer because sea ice keeps the ocean surface temperature close to the melting point (Teng et al. 2006). Thus, the results in a few SH cells during MAM were not statistically significant. The land area showed a decrease in annually averaged temperature, with the largest change of –0.5°C in the middle latitudes over Eurasia (Fig. 3a). The middle latitudes over North America also showed pronounced annual cooling of about –0.2°C. The forcings arising in these regions from prominent deforestation accounted for the cooling, which affects the global climate mainly through changes in SST and sea ice cover. The temperature decreases in northern deforested areas at high latitudes can also be attributed to changes in SSTs and sea ice cover. This cooling favored the expansion of the area of Arctic sea ice, which, in turn, amplified the decrease in temperature through the sea ice–albedo feedback. The lowest amount of cooling of about 0.02°C was at about 30° S; this was also the case for seasonal temperatures (see Fig. 3b–d).

During the spring snow-melt (MAM; Fig. 3b), cooling was significant (but not as substantial as during JJA [June, July and August]; Fig. 3c); the simulation results showed a maximum cooling of 0.5°C over Eurasia and a cooling of about 0.24°C over North America at middle latitudes (when the vegetation–snow–albedo feedback was most notable). A maximum warming effect of 0.05°C was shown at low latitudes over the SH. During the northern summer (JJA; Fig. 3c), the effect of land cover changes was most pronounced at middle northern latitudes, with maximum cooling reaching 0.8°C over Eurasia and 0.28°C over North America. A maximum warming effect of about 0.1°C was shown at low latitudes at this time over the SH (at 25° S). During winter, the maximum cooling response was only 0.25°C, which was smaller than that during spring and summer at middle latitudes over Eurasia (Fig. 3d). A maximum warming effect of about 0.02°C was shown in the SH at this time. Cooling of the NH and warming of the SH were combined results of cooling effects due to albedo increase

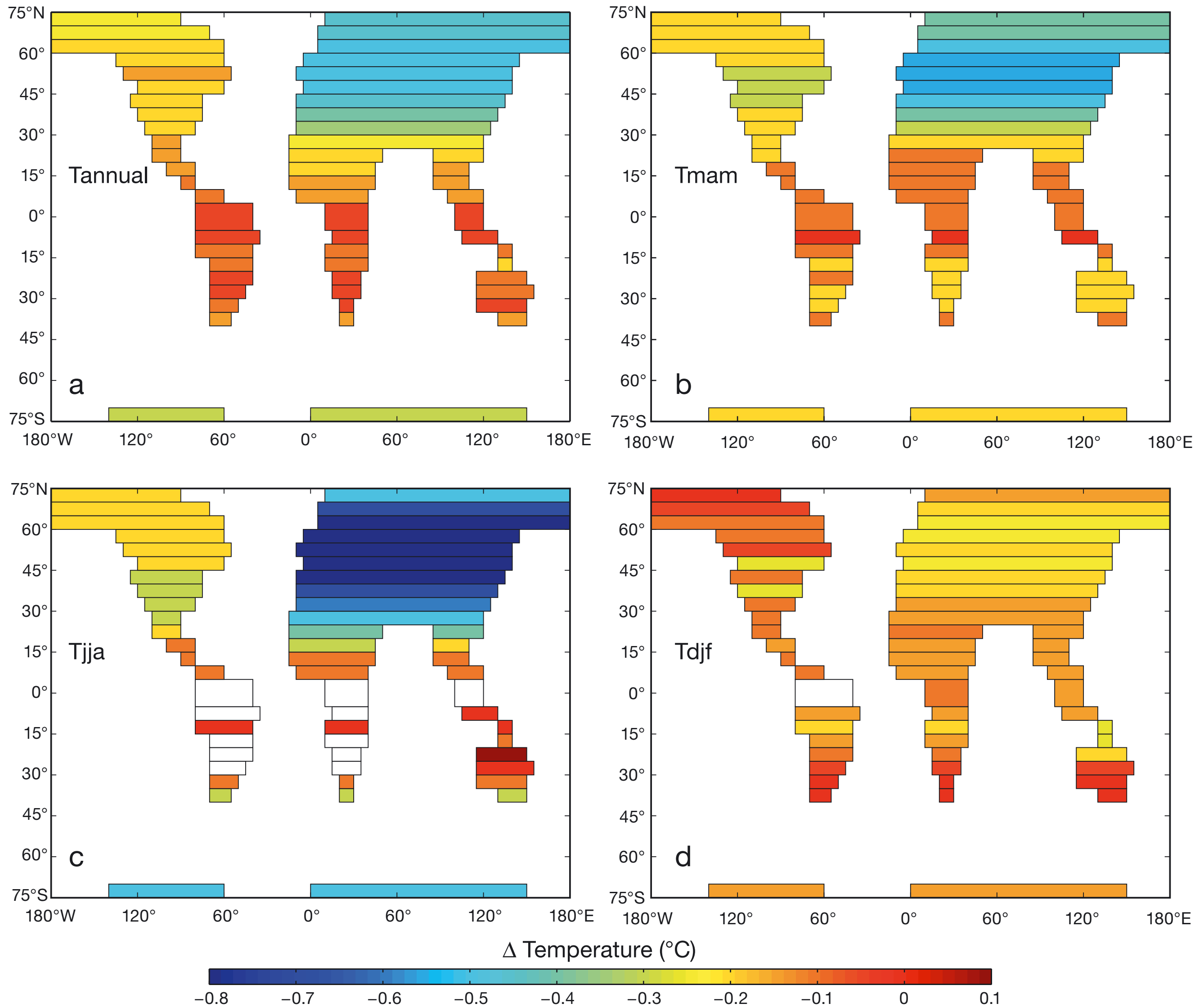

Fig. 3. Average changes in surface air temperature for different seasons: (a) annual (Tannual), (b) March to May (Tmam), (c) June to August (Tjja) and (d) December to February (Tdjf)

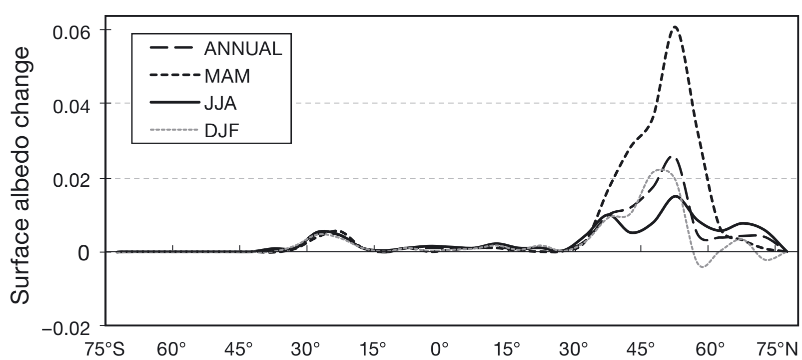

Fig. 4. Zonally averaged changes in land surface albedo in different seasons. MAM: March, April, May; JJA: June, July, August; DJF: December, January, February

and warming effects resulting from precipitation decrease.

The significant cooling at the middle northern latitudes was mostly attributed to changes in land surface albedo (Fig. 4). At middle northern latitudes, the annually averaged maximum albedo was increased by 0.02 (at 50° N) and by <0.01 at the other latitudes (Fig. 4). The strong increase in the albedo corresponded to intense deforestation in this region (see Fig. 1). During spring, the maximum increase in surface albedo was rather high and reached 0.06 (Fig. 4), which suggests that this difference in surface albedo is the main driver behind the significant temperature change (Fig. 3b) in these regions during this part of the year. The albedo changes became smaller during the summer season, since the deforested areas were not snowy and the snow-masking effect of the forest (which increases albedo when there is snow) was therefore absent (Fig. 4). A radiative effect, owing to the higher albedo of grassland relative to forests in the absence of snow, resulted in a land albedo increase of <0.02 in the middle northern latitudes. These data suggest that the surface albedo change was not the main cause of the marked temperature change (Fig. 3c) in this season. During December–February the maximum increase in surface albedo was about 0.02, which was larger than that in summer and smaller than that in spring (Fig. 4). This albedo change had only a moderate effect on temperature because the amount of incoming solar radiation is rather small during winter (see Fig. 3d). There was a maximum increase of <0.01 in surface albedo at 25° S, due to deforestation over the SH.

3.3. The seasonal response of precipitation to historical land cover changes

Since the prominent cooling of historical land cover changes occurred in summer and the maximum surface albedo change was in spring, the precipitation in MAM and JJA which can affect climate through hydrology were analyzed. Zonal differences of average precipitation during the last millennium are given according to season in Fig. 5. The model showed a wavy response. Deforestation led to a reduction in water vapor entering the atmosphere through a decline in the latent heat fluxes. Thus, average precipitation decreased in most regions. Changes in precipitation were smaller in summer than in spring from 40 to 50° N (Fig. 5), with the largest decrease being <0.02 mm d^{-1}. As precipitation decreased, less water was available for evapotranspiration. Deforestation also changed the climate through the warming effect that resulted from a decrease in evapotranspiration. The warming that resulted from reduced evapotranspiration was less during summer than during spring. The cooling due to the increase in albedo in response to deforestation was counteracted slightly by the warming that resulted from reduced evapotranspiration. This was the reason why the maximum cooling was in summer (i.e. there was less of a warming effect from evapotranspiration). Changes in precipitation were greater in summer than in spring in the low latitudes over SH (at 25° S) (Fig. 5), resulting in a greater warming effect in summer than that in spring. This warming effect counteracted the cooling effect owing to high albedos, explaining the warming in the SH. Due to the greater warming effect that resulted from evapotranspiration decrease in summer, there was an increase of 0.1°C in temperature during summer and a less significant warming effect of 0.05°C in spring (Fig. 3).

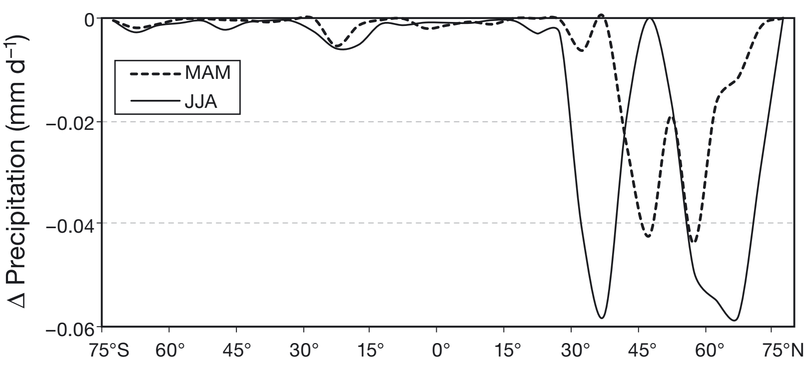

Fig. 5. Zonally averaged changes in surface air precipitation in different seasons. MAM: March, April, May; JJA: June, July, August; DJF: December, January, February

4. DISCUSSION

The MPM-2 simulated a global cooling of 0.13°C due to land cover biogeophysical effects during the last millennium, which was within the range of cooling (−0.05 to 0.39°C) revealed by previous simulations (Betts 2001, Bertrand et al. 2002, Brovkin et al. 2004). On average, the MPM-2 in this study showed a somewhat weaker global response to land cover change than do other EMICs, and GCMs sometimes show a still stronger or even a negative global response. The spread in the response of the MPM-2 and other EMICs is likely caused by different model parameterizations, while the differences among the results between this study and GCM estimates are caused by their components. In comparison with GCMs, MPM-2 embodies the feedbacks and interactions among the components in a climate system by simplifying the courses and details using moderate parameterization. Owing to their interactions, the effects of land cover changes are amplified by feedbacks through other components, particularly those involving hydrology (Brovkin et al. 2006). In addition, radiative forcing is a tool that, in a simple way, can be used to compare different biogeophysical cooling mechanisms. In this paper, the decrease in radiative forcing in response to CERA land cover changes amounted to 0.24 W m^{-2} for the period AD 800–2000. This estimate was well within the range of –0.01 to –0.5 W m^{-2} estimated by previous simulations (Houghton et al. 2001, Myhre & Myhre 2003, Matthews et al. 2004, Goosse et al. 2005, Sitch et al. 2005, Pongratz et al. 2009). Differences among the various estimates may be caused by different parameterizations of the vegetation influence on land surface albedo and different approaches to estimation of radiative forcings in simulations (Brovkin et al. 2006).

Global cooling was simulated due to land cover biogeophysical effects during the last millennium, while the cooling varied according to season. A seasonal cooling occurred in the middle northern latitudes, while a warming occurred in low southern latitudes. The effects of land cover changes were most pronounced in the middle northern latitudes, with maximum cooling reaching approximately 0.8°C during summer due to the smaller decrease of precipitation (that is, less evapotranspiration warming effects) compared to that during spring (Fig. 5), which is in line with some previous simulations. Bonan (1997), using the modified CCM2 model with prescribed SST, revealed that significant summer cooling (2°C) results from land cover changes. The mid-latitude cooling trends are strongly associated with the summer season due to very significant reductions in net radiation at the mid-latitudes (Feddema et al. 2005). The imposed land cover change leads to statistically significant cooling in the NH in summer near-surface temperatures over regions of land cover change (Pitman et al. 2009). Bounoua et al. (2002), in deforestation experiments with a GCM coupled to a SiB2, showed that conversion cools canopy temperatures up to 0.7°C in summer. However, the maximum cooling in summer contradicts results of some AGCM simulations, which show that summer air temperatures increase or have a smaller decrease than in winter and spring (Bonan et al. 1992, Betts 2001). One of the reasons could be that most of the AGCMs were conducted with prescribed SSTs, which modified the global response considerably. Prescribed SSTs neglect the water vapor feedback over the sea surface and may reverse the sign of zonally averaged temperature changes (Ganopolski et al. 2001). In addition, Brovkin et al. (1999), using CLIMBER-2, showed that a maximum cooling of 1.5°C occurs at northern temperate and high latitudes during the spring snow melt, owing to the albedo effect, which is different from the results in this paper. The spread is caused primarily by the CLIMBER-2 model without any flux adjustment between the atmospheric and oceanic modules, which affects the feedbacks among EMICs components and modifies the global response considerably, particularly regarding those components involving sea ice and water vapor. However, the atmosphere module here was represented by a simple energy and moisture balance model in the absence of detailed descriptions about atmospheric circulations and cloud dynamics, so there were still some limitations concerning rainfall in our simulations. Furthermore, the simulation in our study did not involve cloud feedback, which also affects the climate response. In response to surface cooling, most AGCMs simulate an increase in cloud cover which would reduce forcing from deforestation by decreasing the effect of changes in surface albedo on net radiative fluxes at the top of the atmosphere. Due to the absence of the cloud feedback, the climate response was likely to be underestimated in our simulation.

On a global scale, cooling over the SH (25° S) occurred by a maximum of 0.16°C, but the extent of temperature change was dependent on the season. The warming reached 0.05°C during spring, while it was 0.1°C during summer and 0.02°C during winter, due to deforestation at low latitudes of the SH. The seasonal warming of the SH was a combined result of tropical deforestation and changes in atmospheric and oceanic meridional transport of energy. Because of the much smaller land mass area that has been deforested in the SH in comparison to the NH (in Fig. 1), few studies cover temperature change in the SH in detail.

5. CONCLUSIONS

Our study demonstrated that anthropogenic change in land cover has been a substantial factor in climate forcing during the past millennium. Forced by historical land cover changes, MPM-2 revealed a biogeophysical cooling effect of 0.13°C on a global scale. This effect was comparable to the biogeochemical effects from land conversion in previous studies (Brovkin et al. 2004, Matthews et al. 2004). The effect of land cover change was most pronounced over Eurasia, due to its marked replacement of forest with grasslands. A maximum cooling of 0.5°C was noted in the global mean annual temperature over Eurasia at middle latitudes and a minimum cooling of 0.02°C at low latitudes over the SH. Much larger contrasts were found on a seasonal scale; although these changes were largely offset on a yearly scale. A seasonal cooling in the middle northern latitudes and a warming in the low southern latitudes occurred due to historical deforestation. Boreal deforestation led to colder summer temperatures at middle latitudes of the NH. The maximum cooling in the middle latitudes reached approximately 0.8°C over Eurasia during summer, and the maximum warming reached 0.1°C at low latitudes over the SH during this season, while the cooling reached 0.5°C during northern spring and the maximum warming reached 0.05°C at low latitudes over the SH. Our simulations indicated that changes in land cover triggered a chain of feedbacks in the climate system and that these changes had a more pronounced effect on the Earth's climate during summer. The above results highlight the need for further research in this area.

Acknowledgements. This research was supported by a major project of the Chinese National Programs for Fundamental Research and Development (Program 973) (Grant No. 2010CB950903) and the NUAA Foundation (Grant Nos. 1007-909369 and 1007-XNA12078).

LITERATURE CITED

Anav A, Ruti PM, Artale V, Valentini R (2010) Modelling the effects of land-cover changes on surface climate in the Mediterranean region. Clim Res 41:91–104

Avila FB, Pitman AJ, Donat MG, Alexander LV, Abramowitz G (2012) Climate model simulated changes in temperature extremes due to land cover change. J Geophys Res 117:D04108, doi:10.1029/2011JD016382

Bauer E, Claussen M, Brovkin V, Huenerbein A (2003) Assessing climate forcings of the Earth system for the past millennium. Geophys Res Lett 30:1276, doi: 10.1029/2002GL016639

Bertrand C, Loutre MF, Crucifix M, Berger A (2002) Climate of the last millennium: a sensitivity study. Tellus, Ser A, Dyn Meterol Oceanogr 54:221–244

Betts RA (2001) Biogeophysical impacts of land use on present day climate: near-surface temperature and radiative forcing. Atmos Sci Lett 2:39–51

Bonan GB (1997) Effects of land use on the climate of the United States. Clim Change 37:449–486

Bonan GB (1999) Frost followed the plow: impacts of deforestation on the climate of the United States. Ecol Appl 9:1305–1315

Bonan GB, Pollard D, Thompson SL (1992) Effects of boreal forest vegetation on global climate. Nature 359:716–718

Bounoua L, DeFries R, Collatz GJ, Sellers P, Khan H (2002) Effects of land cover conversion on surface climate. Clim Change 52:29–64

Brovkin V, Ganopolski A, Svirezhev Y (1997) A continuous climate-vegetation classification for use in climate-biosphere studies. Ecol Modell 101:251–261

Brovkin V, Ganopolski A, Claussen M, Kubatzki C and others (1999) Modelling climate response to historical land cover change. Glob Ecol Biogeogr 8:509–517

Brovkin V, Sitch S, von Bloh W, Claussen M, Bauer E, Cramer W (2004) Role of land cover changes for atmospheric CO_2 increase and climate change during the last 150 years. Glob Change Biol 10:1253–1266

Brovkin V, Claussen M, Driesschaert E, Fichefet T and others (2006) Biogeophysical effects of historical land cover changes simulated by six Earth system models of intermediate complexity. Clim Dyn 26:587–600

Chase TN, Pielke RA, Kittel TGF, Nemani RR, Running SW (2000) Simulated impacts of historical land cover changes on global climate in northern winter. Clim Dyn 16:93–105

Davin EL, de Noblet-Ducoudré N (2010) Climatic impact of global-scale deforestation: radiative versus nonradiative processes. J Clim 23:97–112

DeFries RS, Bounoua L, Collatz GJ (2002) Human modifications of the landscape and surface climate in the next fifty years. Glob Change Biol 8:438–458

Fanning AF, Weaver AJ (1996) An atmospheric energy–moisture balance model: climatology, interpentadal climate change, and coupling to an ocean general circulation model. J Geophys Res 101:15111–15128

Feddema J, Oleson K, Bonan G, Mearns L, Washington W, Meehl G, Nychka D (2005) A comparison of a GCM response to historical anthropogenic land cover change and model sensitivity to uncertainty in present-day land cover representations. Clim Dyn 25:581–609

Findell KL, Shevliakova E, Milly PCD, Stouffer RJ (2007) Modeled impact of anthropogenic land cover change on climate. J Clim 20:3621–3634

Forest CE, Stone PH, Sokolov AP, Allen MR and others (2002) Quantifying uncertainties in climate system properties with the use of recent climate observations. Science 295:113–117

Ganopolski A, Petoukhov V, Rahmstorf S, Brovkin V and others (2001) CLIMBER-2: a climate system model of intermediate complexity. II. Model sensitivity. Clim Dyn 17:735–751

Gao XJ, Luo Y, Lin WT, Zhao ZC, Giorgi F (2003) Simulation of effects of landuse change on climate in China by a regional climate model. Adv Atmos Sci 20:583–592

Gao XJ, Zhang DF, Chen ZX, Pal JS, Giorgi F (2007) Land use effects on climate in China as simulated by a regional climate model. Sci China D Earth Sci 50:620–628

Goosse H, Renssen H, Timmermann A, Bradley RS (2005) Internal and forced climate variability during the last millennium: a model–data comparison using ensemble simulations. Quat Sci Rev 24:1345–1360

Govindasamy B, Duffy PB, Caldeira K (2001) Land use changes and Northern Hemisphere cooling. Geophys Res Lett 28:291–294

Houghton JT, Ding Y, Griggs DJ, Noguer M and others (2001) Climate change 2001: the scientific basis. Cambridge University Press, Cambridge

Lawrence PJ, Feddema JJ, Bonan GB, Meehl GA and others (2012) Simulating the biogeochemical and biogeophysical impacts of transient land cover change and wood harvest in the community climate system model (CCSM4) from 1850 to 2100. J Climate 25:3071–3095

Matthews HD, Weaver AJ, Meissner KJ, Gillett NP and others (2004) Natural and anthropogenic climate change: incorporating historical land cover change, vegetation dynamics and the global carbon cycle. Clim Dyn 22:461–479

Myhre G, Myhre A (2003) Uncertainties in radiative forcing due to surface albedo changes caused by land-use changes. J Clim 16:1511–1524

Nair US, Ray DK, Wang J, Christopher SA, Lyons T, Welch RM, Pielke RA Sr (2007) Observational estimates of radiative forcing due to land use change in Southwest Australia. J Geophys Res 112:D09117, doi:10.1029/2006JD007505

Otieno VO, Anyah RO (2012) Effects of land use changes on climate in the Greater Horn of Africa. Clim Res 52:77–95

Pielke RA Sr, Pitman A, Niyogi D, Mahmood R and others (2011) Land use/land cover changes and climate: modeling analysis and observational evidence. WIREs Clim Change 2:828–850

Pitman AJ, de Noblet-Ducoudré N, Cruz FT, Davin EL and others (2009) Uncertainties in climate responses to past land cover change: first results from the LUCID intercomparison study. Geophys Res Lett 36, doi:10.1029/2009GL039076

Pitman AJ, Avila FB, Abramowitz G, Wang YP, Phipps SJ, de Noblet-Ducoudré N (2011) Importance of background climate in determining impact of land-cover change on regional climate. Nature Climate Change 1:472–475

Pongratz J, Reick C, Raddatz T, Claussen M (2008) A reconstruction of global agricultural areas and land cover for the last millennium. Global Biogeochem Cycles 22:GB3018, doi:10.1029/2007GB003153

Pongratz J, Raddatz T, Reick CH, Esch M, Claussen M (2009) Radiative forcing from anthropogenic land cover change since A.D. 800. Geophys Res Lett 36:L02709, doi:10.1029/2008GL036394

Semtner AJ (1976) A model for the thermodynamic growth of sea ice in numerical investigations of the climate. J Phys Oceanogr 6:379–389

Sitch S, Brovkin V, von Bloh W, van Vuuren D, Eickhout B, Ganopolski A (2005) Impacts of future land cover changes on atmospheric CO_2 and climate. Global Biogeochem Cycles 19:GB2013, doi:10.1029/2004GB002311

Teng H, Warren M, Washington GA, Meehl GA, Lawrence EB, Strand GW and others (2006) Twenty-first century Arctic climate change in the CCSM3 IPCC scenario simulations. Clim Dyn 26:601–616

Wang Y, Lawrence AM, Wang Z, Brovkin V (2005) The greening of the McGill paleoclimate model. II. Simulation of Holocene millennial-scale natural climate changes. Clim Dyn 24:481–496

Wang Z, Mysak LA (2000) A simple coupled atmosphere-ocean–sea ice-land surface model for climate and paleoclimate studies. J Clim 13:1150–1172

Wang Z, Mysak LA (2001) Ice sheet-thermohaline circulation interactions in a climate model of intermediate complexity. J Oceanogr 57:481–494

Wang Z, Mysak LA, McManus JF (2002) Response of the thermohaline circulation to cold climates. Paleoceanography 17, doi:10.1029/2000PA000587

Wang Z, Cochelin ASB, Lawrence AM, Wang Y (2005) Simulation of the last glacial inception with the green McGill paleoclimate Model. Geophys Res Lett 32:L12705, doi:10.1029/2005GL023047

Zhang JY, Dong WJ, Fu CB (2005) Impact of land surface deg-radation in northern China and southern Mongolia on regional climate. Chin Sci Bull 50:75–81

Zwiers FW, von Storch H (1995) Taking serial correlation into account in tests of the mean. J Clim 8:336–351

Editorial responsibility: Gouyu Ren, Beijing, PR China

Submitted: June 5, 2012; Accepted: January 15, 2013
Proofs received from author(s): March 14, 2013